Predicting the soil water characteristic curve from the particle size distribution based on a pore space geometry containing slit-shaped spaces

Chen-chao Chang, Dong-hui Cheng

School of Environmental Sciences and Engineering, Chang'an University, Xi'an, 710054, China;
Key Laboratory of Subsurface Hydrology and Ecological Effects in Arid Region (Chang'an University), Ministry of Education, Xi' an, China

Correspondence to: Dong-hui Cheng (chdhbsh@chd.edu.cn)

Abstract. Traditional models employed to predict the soil water characteristic curve (SWC) from the particle size distribution (PSD) always underestimate the water content in the dry range of the SWC. Using the measured physical parameters of 48 soil samples from the UNSODA unsaturated soil hydraulic property database, these errors were proven to originate from the underestimation of the pore volume fraction of the minimum pore diameter range. A method was therefore proposed to improve the estimation of the water content in the high suction range using a pore model comprising a circle-shaped central pore connected to slit-shaped spaces; in this model, the pore volume fraction of the minimum pore diameter range and the corresponding water content were accordingly increased. The SWCs predicted using the improved method reasonably approximated the measured SWCs, and which were more accurate than those obtained using traditional method in the dry range of the SWC.

1 Introduction

The soil water characteristic curve (SWC), which represents the relationship between the water pressure and water content, is fundamental to researching water flow and chemical transport in unsaturated media (Pollacco et al., 2017). Direct measurements of the SWC consume both time and money (Arya and Paris, 1981;Mohammadi and Vanclooster, 2011), while estimating the SWC from the particle size distribution (PSD) is both rapid and economical. Therefore, a number of associated conceptual and physical models have been proposed.

The first attempt to directly translate a PSD into an SWC was performed by Arya and Paris (1981) (hereinafter referred to as the AP model). In this model, the PSD is divided into multiple size fractions and the bulk and particle densities of the natural-structure sample are uniformly applied to each particle size fraction, from which it follows that the relative pore fraction and the relative solid fraction are equal. Thus, the degree of saturation can be set equal to the cumulative PSD function. The soil suction head can be obtained using the capillary equation based on a "bundle of cylindrical tubes" model, and the pore size in the equation is determined by scaling the pore length and pore volume (Arya et al., 2008). Based on the

principle of the AP model, many researchers have focused on improving the suction head calculations, which are commonly based on the capillary equation; however, various methods are used to translate the particle diameter into the pore diameter (Haverkamp et al., 1986;Zhuang et al., 2001;Mohammadi and Vanclooster, 2011;Jensen et al., 2015). Some models estimate the pore diameter based on particle packing patterns (e.g., the MV model), while others utilize the proportionality factor

5 between the pore size and the associated particle diameter (e.g., the HP model and two-stage approach). However, the scheme employed to estimate the water content has not been modified and follows the approach of the AP model.

However, these traditional models which follow the water content calculation approach of the AP model underestimate the water content in the dry range of the SWC (Hwang and Powers, 2003;Meskini-vishkaee et al., 2014). Therefore, some researchers have attempted to improve the water content calculation approach by attributing model errors to both a

10 simplified pore geometry and an incomplete desorption of residual water in the soil pore within the high matric suction head range (Tuller et al., 1999;Mohammadi and Meskini-Vishkaee, 2012). Recent findings revealed the existence of corner water, lens water and film water in soils at high matric suction head (Tuller et al., 1999;Mohammadi and Meskini-Vishkaee, 2012;Or and Tuller, 1999;Shahraeeni and Or, 2010;Tuller and Or, 2005). Therefore, Mohammadi and Meskini-Vishkaee (2012) slightly improved upon the traditional MV model and predicted the SWC based on the PSD while considering

15 adsorbed water film and lens water between the soil particles. Tuller et al. (1999) proposed a pore space geometry containing slit-shaped spaces and derived a corresponding SWC that considered water film and water in angular-shaped pores; however, the SWC failed to describe experimental data at an intermediate water content due to the limitations of the gamma distribution function used to characterize the pore size distribution (PoSD) (Lebeau and Konrad, 2010). Moreover, this model was mathematically complex. Mohammadi and Meskini-Vishkaee (2013) incorporated the residual water content into

20 the MV model and consequently decreased the magnitude of the underestimation in the dry range of the SWC. However, an accurate estimation of the residual water content remains a challenge.

Many traditional models are based on a "bundle of cylindrical tubes" representation of the pore space geometry (Arya and Paris, 1981;Zhuang et al., 2001), which results in intrinsic errors when predicting water flow in variably saturated soils. Consequently, some researchers have considered pore networks as bundles of triangular tubes, which could incorporate the

25 contribution of water in pore corners to the water content (Helland and Skjæveland, 2007). A new pore geometry model comprising a polygon-shaped central pore connected to slit-shaped spaces was proposed by Tuller et al. (1999) to provide a more realistic representation of natural pore spaces (Tuller et al., 1999;Or and Tuller, 1999;Tuller and Or, 2001). This model could represent a foundation for accurately describing the water status in natural soils, particularly in arid environments.

The objectives of this study were therefore to evaluate the leading factors that lead to the underestimation of the water

30 content in the dry range of the SWC using traditional methods and to furthermore propose a method for accurately estimating the water content using a pore space geometry containing slit-shaped spaces to improve the prediction of the SWC.

2 Basic descriptions

The relationship between the PSD and the PoSD is a fundamental element when predicting the SWC from the PSD. Hwang and Powers (2003) found that the nonlinear relationship between the PSD and the PoSD would be more appropriate than the linear relationship applied in the AP model and therefore described both the PSD and the PoSD as lognormal distributions.

5 However, since the PSD and PoSD of soils do not strongly follow a lognormal distribution, this model performed very poorly for moderately fine-textured soils (Hwang and Choi, 2006). Obtaining an accurate PoSD from the PSD of a soil is highly difficult, and the errors that arise from this approach could cause inevitable errors in the SWC. However, the underestimation of the water content in the dry range of an SWC has not been comprehensively evaluated from this perspective.

10 In this study, the measured PoSDs of 48 soil samples were compared with the PoSDs calculated using a traditional model (They were actually corresponding PSDs) to identify the origins of the errors and their effects on the accuracy of the SWC. The provided 48 soil samples exhibited a wide range of physical properties (Table 1), and they were selected from the UNSODA unsaturated soil hydraulic property database, which contains 790 soil samples with general unsaturated soil hydraulic properties and basic soil properties (e.g., water retention, hydraulic conductivity, soil water diffusivity, PSD, bulk

15 density, and organic matter content) (Nemes et al., 2001).

(1) Calculating the PoSD using a traditional model

Traditional models commonly assume that the pore volume fraction of each size fraction can be set equal to the relative solid fraction(Arya and Paris, 1981). Thus, the cumulative pore volume fraction can take the following form:

$$\sum_{j=1}^{j=i} v_i = \sum_{j=1}^{j=i} \omega_i; \quad i = 1, 2, 3, \cdots, n \tag{1}$$

20 where ω_i is the solid fraction of the ith particle fraction, v_i is the pore volume fraction associated with the ith fraction, and n is the total number of size fractions in the PSD.

The routine procedures employed among the several traditional models to translate a particle diameter into a pore diameter are different. The equivalent pore diameter can be derived from physical properties, including the bulk density and the particle density, or from the proportionate relationship between the pore size and associated particle diameter. Although the former can logically characterize a pore, a complicated pattern can slightly reduce the model performance. Meanwhile, the

25 latter approach is easy to use, and its rationality has been demonstrated by some researchers (Hamamoto et al., 2011;Sakaki et al., 2014). Here, the latter technique was applied, and it can be expressed as

$$d_i = 0.3 D_i \tag{2}$$

where D_i is the mean particle diameter of the ith fraction (μm), d_i is the corresponding equivalent pore diameter (μm).

30 Inputting the PSD data, then calculated pore diameters are sequentially paired with corresponding pore volume fractions to obtain a Calculated PoSD.

(2) Measuring the PoSD

It is generally difficult to measure the PoSD of a soil; however, the PoSD can be indirectly obtained using the measured water content and suction head (Jayakody et al., 2014). The cumulative pore volume fraction of the ith fraction is equal to the ratio of the measured water content to the saturated water content (Eq. (3)):

$$\theta_i = \theta_s \sum_{j=1}^{j=i} v_j; \quad i = 1, 2, 3, \cdots, n \tag{3}$$

where θ_s is the saturated water content (cm^3 cm^{-3}), and θ_i is the measured water content (cm^3 cm^{-3}). Meanwhile, the corresponding pore diameters are derived on the basis of capillary theory and Eq. (4).

$$\psi_i = \frac{3000}{d_i} \tag{4}$$

where ψ_i is suction head (cmH$_2$O). The PoSD obtained in this way is considered the measured PoSD.

The calculated and measured PoSD data were fitted using a modified logistic growth model (Eq. (5)) (Liu et al., 2003):

$$w_i = \frac{1}{1 + a \exp\left(-b d_i^c\right)} \tag{5}$$

where w_i is the cumulative pore volume fraction with diameters smaller than d_i (%), and a, b, and c are the fitting parameters (dimensionless). This model produced a good fit for the PoSD data employed in this study with a coefficient of determination (r^2) that ranged from 0.972 to 0.999.

The measured pore volume fraction curves for the typical samples, namely, sand (code: 3172) and clay (code: 2360), and their calculated curves using the traditional model are presented in Fig. 1. The small maps embedded in Fig. 1 exhibit the measured and calculated PoSD curves. Figure 1 show that the calculated PoSD curves approximately coincide with the measured curves in the larger pore diameter range, while the calculated values in the smaller range, which correspond to the higher suction range on the SWC curve, are obviously smaller than the measured values. The underestimation of the PoSD in the smaller pore diameter range can consequently lead to an underestimation of the water content at a higher suction range. In particular, the calculated pore volume fraction associated with the smallest pore diameter ($d \leq 0.6$ μm) was far less than the measured pore fraction. These results illustrate that the underestimation of the pore volume fraction with respect to the smallest pore diameter ($d \leq 0.6$ μm) was a key factor with regard to the underestimation of the water content in the dry range of the SWC. Besides, the underestimation of pore volume fraction is associated with an oversimplified pore space geometry, which traditional models have generally characterized as a bundle of cylindrical capillaries. The measured and calculated pore curves of the other 46 soil samples behaved in the same fashion, and those curves are provided in the supporting information (Fig. S1).

3 Improved method

3.1 Estimating the pore volume fraction

In this study, the soil pore structure is conceptualized within a pore model in which the elementary unit cell is composed of a relatively larger circle-shaped central pore connected to two slit-shaped spaces (see Fig. 2). Relative to the polygonal central

5 pore connected to slit-shaped spaces as described by Or and Tuller (1999), both the slit width and the slit length are proportional to the diameter of the associated central pore d and are therefore expressed as αd and βd, respectively.

When estimating the pore volume fraction using the pore model described above, the volume fractions of the central pore and slit-shaped space are distinguished. The slit-shaped pore spaces are accordingly classified into the smallest central pore size since the sizes of the slit-shaped pore spaces are smaller than the minimum central pore diameter. The particle sizes of

10 our samples range from 2 to 2000 μm, and the corresponding pore sizes are between 0.6 and 600 μm; meanwhile, the largest slit width calculated from the parameters in Table 2 is 0.24 μm. In addition, when the drainage potential is given as μ=-$2\sigma/(\rho\alpha d)$ based on the capillary theory (Derjaguin and Churaev, 1992), the critical potential for slit snap-off of the widest slit is 6202 cm, which is smaller than the critical potential of 5000 cm calculated using Eq. (4) for the minimum central pore. This also demonstrates that the equivalent pore diameter of a slit space is smaller than the minimum central pore diameter.

15 Therefore, the pore volume fractions of the soil samples were simplified into those of central pores, but the volume fraction of the minimum central pore contained the volume fraction of all slit-shaped spaces. Coupled with the traditional assumption that the volume fraction of each unit cell (i.e., the central pore and two slit spaces) is equal to the relative particle mass fraction and the geometric relationship described in Fig. 2, the volume fractions of central pores and slit-shaped space can be separated, then the pore volume fractions with respect to different sizes can be readily obtained.

20 The procedure utilized to calculate the pore volume fraction is shown in Fig. 3. Assuming that the soil pores are composed of numerous unit cells with various sizes, the fraction of the ith unit cell is equal to the relative particle mass fraction ω_i. The sum of the slit pore volume fractions of various sizes ($\zeta_2+\zeta_3+\ldots\ldots+\zeta_i$) and the volume fraction of the smallest unit cell (ω_1) form the volume fraction of the smallest pore (v_1). Successively accumulating that volume fraction with the other central pore volume fractions (i.e., v_2, v_3, v_4…) provides the PoSD of a sample. The slit pore volume fraction, ζ_i, the volume fraction

25 of the smallest pore v_1 and the volume fractions of the other pores v_i were calculated using Eq. (6), Eq. (7) and Eq. (8), respectively:

$$\zeta_i = \omega_i \frac{2\alpha\beta d_i^2}{2\alpha\beta d_i^2 + \frac{\pi}{4} d_i^2} \tag{6}$$

$$v_1 = \omega_1 + \sum_2^n \zeta_i \tag{7}$$

$$v_i = \omega_i - \zeta_i \qquad (8)$$

where ζ_i is the slit pore volume fraction, v_i is the volume fraction of the ith pore fraction, and α and β are the scaling parameters of the slit width and the slit length, respectively.

3.2 Values of α and β

5   To obtain the values of α and β, an expression containing both of these parameters with respect to the specific surface area (S_{SA}) was applied here. The S_{SA} of the pore as shown in Fig. 2 can be described using a geometrical relationship as follows:

$$S_{SA} = \frac{\phi}{1000\rho_b} \sum_{j=1}^{i=j} \omega_i \frac{4\beta d_i + \pi d_i}{2\alpha\beta d_i^2 + \frac{\pi}{4} d_i^2}; \quad i = 1, 2, \cdots n \qquad (9)$$

where S_{SA} is the specific surface area (m^2 g^{-1}), d_i is the pore diameter (m), ρ_b is the bulk density (kg m^{-3}) and Φ is the

10   measured porosity. Therefore, an important requirement for the calculation of the α and β values is an estimate of the sample-scale value of S_{SA}. Here, a power equation was applied as follows (Sepaskhah et al., 2010):

$$S_{SA} = 3.89 d_g^{-0.905} \qquad (10)$$

where S_{SA} is the estimated specific surface area (m^2 g^{-1}), and d_g is the geometric mean particle size diameter (mm) obtained using Eq. (11) (Shirazi and Boersma, 1984):

15   $$d_g = \exp\left(f_c \ln M_c + f_{si} \ln M_{si} + f_{sa} \ln M_{sa}\right) \qquad (11)$$

where f_c, f_{si} and f_{sa} are the clay, silt and sand fractions (%) of the soil sample, respectively, M_c, M_{si} and M_{sa} are the mean diameters of clay, silt and sand that are empirically taken as 0.001 mm, 0.026 mm and 1.025 mm, respectively.

Consequently, the quantitative relationship between the parameters α and β can be obtained using Eq. (9). Associated with the additional constraint of Eq. (10), the values of α and β can be theoretically solved if the measured slit volume fraction or

20   the measured SWC is known. However, an analytical solution is difficult to derive due to the high nonlinearity of both equations. Here, a trial and error approach was adopted that was much easier than the analytical method. Conveniently, UNSODA database provided a great deal of soil information, including measured SWCs and diverse physical properties.

The routine procedure for handling a soil sample involved the following steps. First, given the initial value of α, the value of β was calculated using Eqs. (9)-(11), after which the PoSD was predicted using Eqs. (6)-(8). Subsequently, the SWC was

25   estimated using the method described in Sect. 3.3. Finally, the value of α was changed repeatedly until the newer predicted SWC was in good agreement with the measured SWC and the water content corresponding to a suction head of 5000 cmH$_2$O was within 90% of the measured data (see Fig.S2 in the supporting information). The results for the 48 soil samples indicated that the β values exhibited a broad range of variation for all samples, while the α values showed regular changes

with the soil texture. The relationship between the sand contents and α values for the 48 samples is shown in Fig. 4, which clearly demonstrates that the values of α are similar for samples with specific sand contents.

Therefore, the approach was simplified by setting α as a constant for similar soil textures. The corresponding detailed descriptions are summarized in Table 2. The values of α were in the range from 3.34E-05 to 2.12E-02, which were estimated by Or and Tuller (1999) using a pore-scale geometry model comprising a polygon-shaped central pore connected to slit-shaped spaces. According to the sand contents, Table 2 is a reference for determining the α values for sample that serve as input parameters in predicting the SWC from the PSD hereinafter.

3.3 Estimating the SWC

The values of α and β for the various soil samples facilitated the acquisition of the volume fractions of the slit pores using Eq. (6) and the PoSD using Eqs. (7) and (8). The water contents associated with different pore filling stages could be estimated by substituting the PoSD into Eq. (3), and the pore sizes and the corresponding suction heads could be calculated using Eqs. (2) and (4). The SWC could be ultimately obtained using the calculated suction heads and water contents.

4 Model validation

4.1 Data sources

Twenty-two soil samples with a wide range of physical properties were also selected from UNSODA database to validate the model; the codes and contents of the samples are summarized in Table 3 and Fig. 5. For the soil samples that were not provided with a saturated water content θ_s, the first data point of the measured SWC corresponding to the lowest suction head was regarded as θ_s.

To generate a detailed PSD, a modified logistic growth model (Eq. (5)) was used to fit the measured PSD data. Here, the detailed PSD was generated at diameter classes of 2, 5, 10, 15, 20, 30, 40, 50, 60, 70, 80, 90, 100, 200, 500, 1000 and 2000 μm. The values of α were obtained according to the sand contents of samples, the details of which are included in Table 2. The values of β were obtained by substituting the S_{SA} values predicted using Eq. (10) into Eq. (9). Then, the PoSD was predicted using Eqs. (6)-(8). Finally, the SWC was estimated using the methods described in Sect. 3.3.

The SWC was also predicted using the traditional method presented in Sect. 2. In the traditional method, the predicted PoSD was equivalent to the PSD in Eq. (1) and was substituted into Eq. (3) to obtain the water content. The corresponding suction heads were predicted using Eqs. (2) and (4).

The van Genuchten equation (Eq. (12)) was used to fit the SWC data calculated via the traditional method and the improved method (Genuchten, 1980):

$$\frac{\theta - \theta_r}{\theta_s - \theta_r} = \left[\frac{1}{1 + (a\psi)^n}\right]^m \tag{12}$$

where θ is the water content (cm^3 cm^{-3}), θ_r is the residual water content (cm^3 cm^{-3}), and a, n, m, and θ_r are fitting parameters. The 22 samples exhibited good fits with an average r^2 value of greater than 0.999.

For each set of predictions, the agreement between the predicted water content θ_p and the measured moisture content θ_m was
expressed in terms of the root mean square error (E_{RMS}), which is given by

$$E_{RMS} = \sqrt{\frac{1}{N}\sum_{i=1}^{N}(\theta_p - \theta_m)^2} \tag{13}$$

where N is the number of measured data points.

4.2 Results

The predicted and measured SWCs in Fig. 6 show that the improved method exhibited good fits with the measured data in the entire range of the SWC; moreover, the proposed method is clearly better than the traditional method, especially at the dry range (the other 18 samples are listed in Fig.S3 in the supporting information). The E_{RMS} values range from 0.017 to 0.054 for the improved method (with an average of 0.027) and from 0.040 to 0.106 for the traditional method (with an average of 0.057), thereby demonstrating that the improved method performed better than the traditional method (Table 4).

The accuracy of an SWC predicted using the improved method depends on the accuracy of the corresponding predicted pore volume fraction. The calculated and measured pore volume fraction curves in Fig. 6 indicate that the predicted pore volume fraction curves using the improved method are more similar to the measured data than those predicted using the traditional method, thereby showing that the proposed method performed better. The errors in the predicted pore fraction using the traditional method mainly occur at the minimum pore size ($d \leq 0.6$ μm), while the proposed method greatly improves the volume fraction at the minimum pore size and consequently improves the water content in the high suction range. These improvements are mainly attributed to the pore model containing slit-shaped spaces, demonstrating that this pore model is better for predicting the SWC from the PSD than the concept of a bundle of cylindrical tubes.

4.3 Discussions

4.3.1 The effects of estimated S_{SA} values

The S_{SA} values estimated using Eq. (10) could affect the accuracy of the predicted SWC. Fig. 7 shows that an overestimation of the S_{SA} would prompt the dry range of the SWC curve to move in the direction of a larger water content, and vice versa. When the estimated error in the S_{SA} was ±20% of its accurate value, a relatively small error appeared between the calculated and measured SWCs. When the estimated S_{SA} value was altered by 10% and -10% of its accurate value for the loamy sand (code: 3170), the water contents with respect to the highest suction head were higher and lower, respectively, by

approximately 0.007 cm^3 cm^{-3} than those of the original SWC. For the clay (code: 4680), the water contents were higher and lower by approximately 0.009 cm^3 cm^{-3} at the same 10% and -10% alterations, respectively. Consequently, for the coarse-textured soil, the water content and prediction error of the SWC changed relatively little for the same degree of change of the S_{SA}.

5   Previous work showed that the S_{SA} of soil is closely dependent upon the soil texture and that it could be estimated from the soil media data and PSD (Sepaskhah and Tafteh, 2013;Resurreccion et al., 2015). The method used to estimate the S_{SA} in Sect. 3.2 was presented by Sepaskhah et al. (2010), who estimated the S_{SA} based on the geometric mean particle size diameter as shown in Eq. (10) with an r^2 value of 0.88. Moreover, the appropriateness of this equation was validated using 64 soil samples by Fooladmand (2011). Therefore, this equation is capable of estimating the S_{SA}, but more effort should be

10   directed toward developing a more accurate transformation from soil physical properties to S_{SA} to improve the prediction of the SWC.

4.3.2 Physical meanings of the parameters

Since the central pore diameter d is proportional to the corresponding particle diameter D, the slit width αd, slit length βd and specific surface area S_{SAi} of each unit cell are associated with the particle size. The calculated values of αd, βd and S_{SAi} of

15   clay, silt, fine sand and coarse sand particles for the loamy sand (code: 3170) are listed in Fig. 8. The results confirm that pores formed by bigger soil particles are large with a correspondingly large slit width αd; this is similar to the results in Or and Tuller (1999), and the values are of the same order of magnitude. It is common knowledge that larger soil particles tend to have large surface areas, and therefore, the slit length formed by the contact of soil particle edges should be relatively long, leading to the positive relationship between the slit length βd and the particle diameter as shown in Fig. 8. This result is

20   different from that in Or and Tuller (1999), where the slit length βd was inversely proportional to the particle diameter. In addition, the S_{SAi} of the ith particle fractions decrease with an increase in the particle diameter, which is consistent with the findings of Or and Tuller (1999) and is in accordance with the general understanding of the S_{SA}.

5 Conclusions

The traditional models employed to translate the PSD into the SWC underestimate the water content in the dry range of the

25   SWC. The errors originating from an underestimation of the pore volume fraction of the minimum pore diameter range in traditional methods are the result of setting the cumulative PoSD equal to the corresponding PSD. The pore volume fraction of the minimum pore diameter range will be accordingly increased if the slit-shaped pore spaces are taken into consideration when estimating PoSD with a pore model comprising a circle-shaped central pore connected to slit-shaped spaces; therefore, the SWC can be more accurately predicted from the PSD. The estimation of the α and β parameters is a key step for

30   predicting the SWC in the proposed method. The α values were obtained using 48 measured soil samples, and those values served as input parameters while predicting the SWC; then, the β values were readily calculated using a constraint on the S_{SA}.

The results of the model validation illustrated that the SWCs predicted using the proposed method demonstrated a good fit with the measured data and the proposed method performed better than the traditional method, especially in the dry range of the SWC.

5 *Competing interests.* The authors declare that they have no conflicts of interest.

Acknowledgments and data

The research was funded by the Special Fund for Basic Scientific Research of Central Colleges, Chang'an University (310829162015). The authors thank Kang Qian for providing the UNSODA unsaturated soil hydraulic property database.

References

Arya, L. M., and Paris, J. F.: A physicoempirical model to predict the soil moisture characteristic from particle-size distribution and bulk density, Soil Science Society of America Journal, 45, 1023-1030, doi:10.2136/sssaj1981.03615995004500060004x, 1981.

Arya, L. M., Bowman, D. C., Thapa, B. B., and Cassel, D. K.: Scaling soil water characteristics of golf course and athletic field sands from particle-size distribution, Soil Science Society of America Journal, 72, 25-32, doi:10.2136/sssaj2006.0232, 2008.

Derjaguin, B. V., and Churaev, N. V.: Polymolecular adsorption and capillary condensation in narrow slit pores, Progress in Surface Science, 40, 173-191, doi: 10.1016/0079-6816(92)90045-J, 1992.

Fooladmand, H. R.: Estimating soil specific surface area using the summation of the number of spherical particles and geometric mean particle-size diameter, African Journal of Agricultural Research, 6(7), 1758-1762, doi: 10.5897/AJAR11.199, 2011.

Genuchten, M. T. V.: A closed-form equation for predicting the hydraulic conductivity of unsaturated soils, Soil Science Society of America Journal, 44, 892-898, doi:10.2136/sssaj1980.03615995004400050002x, 1980.

Hamamoto, S., Moldrup, P., Kawamoto, K., Jonge, L. W. D., Schjønning, P., and Komatsu, T.: Two-region extended archie's law model for soil air permeability and gas diffusivity, Soil Science Society of America Journal, 75(3), 795-806, doi: 10.2136/sssaj2010.0207, 2011.

Haverkamp, R., Parlange, and J., Y.: Predicting the water-retention curve from particle-size distribution: 1. sandy soils without organic matter1, Soil Science, 142, 325-339, 1986.

Helland, J. O., and Skjæveland, S. M.: Relationship between capillary pressure, saturation, and interfacial area from a model of mixed‐wet triangular tubes, Water Resources Research, 43, 398-408, doi: 10.1029/2006WR005698, 2007.

Hwang, S. I., & Powers, S. E.: Using particle-size distribution models to estimate soil hydraulic properties. Soil Science Society of America Journal, 67(4), 1103-1112, doi:10.2136/sssaj2003.1103, 2003.

Hwang, S. I., and Choi, S. I.: Use of a lognormal distribution model for estimating soil water retention curves from particle-size distribution data, Journal of Hydrology, 323, 325-334, doi: 10.1016/j.jhydrol.2005.09.005, 2006.

Jayakody, K. P. K., Shimaoka, T., Komiya, T., and Ehler, P.: Laboratory determination of water retention characteristics and pore size distribution in simulated MSW landfill under settlement, International Journal of Environmental Research, 8, 79-84, 2014.

Jensen, D. K., Tuller, M., Jonge, L. W. D., Arthur, E., and Moldrup, P.: A new Two-Stage Approach to predicting the soil water characteristic from saturation to oven-dryness, Journal of Hydrology, 521, 498-507, doi: 10.1016/j.jhydrol.2014.12.018, 2015.

Lebeau, M., and Konrad, J. M.: A new capillary and thin film flow model for predicting the hydraulic conductivity of unsaturated porous media, Water Resources Research, 46, W12554, doi:10.1029/2010WR009092, 2010.

Liu, J. L., Xu, S. H., and Liu, H.: Investigation of different models to describe soil particle-size distribution data, Advances in Water Science, doi: 10.3321/j.issn:1001-6791.2003.05.010, 2003.

Meskini-vishkaee, F., Mohammadi, M. H., and Vanclooster, M.: Predicting the soil moisture retention curve, from soil particle size distribution and bulk density data using a packing density scaling factor, Hydrology & Earth System Sciences, 18, 4053-4063, doi: 10.5194/hess-18-4053-2014, 2014.

Mohammadi, M. H., and Vanclooster, M.: Predicting the soil moisture characteristic curve from particle size distribution with a simple conceptual model, Vadose Zone Journal, 10(2), 594-602, doi:10.2136/vzj2010.0080, 2011.

Mohammadi, M. H., and Meskini-Vishkaee, F.: Predicting the film and lens water volume between soil particles using particle size distribution data, Journal of Hydrology, 475, 403-414, doi:10.1016/j.jhydrol.2012.10.024, 2012.

Mohammadi, M. H., and Meskini-Vishkaee, F.: Predicting soil moisture characteristic curves from continuous particle-size distribution data, Pedosphere, 23, 70-80, doi: 10.1016/S1002-0160(12)60081-2, 2013.

5 Nemes, A., Schaap, M. G., Leij, F. J., and Wösten, J. H. M.: Description of the unsaturated soil hydraulic database UNSODA version 2.0, Journal of Hydrology, 251, 151-162, doi: 10.1016/S0022-1694(01)00465-6, 2001.

Or, D., and Tuller, M.: Liquid retention and interfacial area in variably saturated porous media: Upscaling from single‐pore to sample‐scale model, Water Resources Research, 35, 3591-3605, doi: 10.1029/1999WR900262, 1999.

Pollacco, J. A. P., Webb, T., Mcneill, S., Hu, W., Carrick, S., Hewitt, A., and Lilburne, L.: Saturated hydraulic conductivity model 10 computed from bimodal water retention curves for a range of New Zealand soils, Hydrology & Earth System Sciences, 21, 1-27, doi: org/10.5194/hess-21-2725-2017, 2017.

Resurreccion, A. C., Moldrup, P., Tuller, M., Ferré, T. P. A., Kawamoto, K., Komatsu, T., and Jonge, L. W. D.: Relationship between specific surface area and the dry end of the water retention curve for soils with varying clay and organic carbon contents, Water Resources Research, 47, 240-250, doi: 10.1029/2010WR010229, 2015.

15 Sakaki, T., Komatsu, M., and Takahashi, M.: Rules-of-Thumb for predicting air-entry value of disturbed sands from particle size, Soil Science Society of America Journal, 78, 454, doi:10.2136/sssaj2013.06.0237n, 2014.

Sepaskhah, A. R., Tabarzad, A., and Fooladmand, H. R.: Physical and empirical models for estimation of specific surface area of soils, Archives of Agronomy & Soil Science, 56, 325-335, doi: 10.1080/03650340903099676, 2010.

Sepaskhah, A. R., and Tafteh, A.: Pedotransfer function for estimation of soil-specific surface area using soil fractal dimension of 20 improved particle-size distribution, Archives of Agronomy and Soil Science, 59, 1-11, doi: 10.1080/03650340.2011.602632, 2013.

Shahraeeni, E., and Or, D.: Pore-scale analysis of evaporation and condensation dynamics in porous media, Langmuir the Acs Journal of Surfaces & Colloids, 26, 13924-13936, doi: 10.1021/la101596y, 2010.

Shirazi, M. A., and Boersma, L.: A unifying quantitative analysis of soil texture, Soil Science Society of America Journal, 48, 142-147, doi: 10.2136/sssaj1984.03615995004800010026x, 1984.

25 Tuller, M., Or, D., and Dudley, L. M.: Adsorption and capillary condensation in porous media: Liquid retention and interfacial configurations in angular pores, Water Resources Research, 35, 1949–1964, doi: 10.1029/1999WR900098, 1999.

Tuller, M., and Or, D.: Hydraulic conductivity of variably saturated porous media: Film and corner flow in angular pore space, Water Resources Research, 37, 1257-1276, doi: 10.1029/2000WR900328, 2001.

Tuller, M., and Or, D.: Water films and scaling of soil characteristic curves at low water contents, Water Resources Research, 41, 319-335, 30 doi: 10.1029/2005WR004142, 2005.

Zhuang, J., Jin, Y., and Miyazaki, T.: Estimating water retention characteristic from soil particle-size distribution using a non-similar media concept, Soil Science, 166, 308-321, doi: 0038-075C/01/16605-308–321, 2001.

35

40
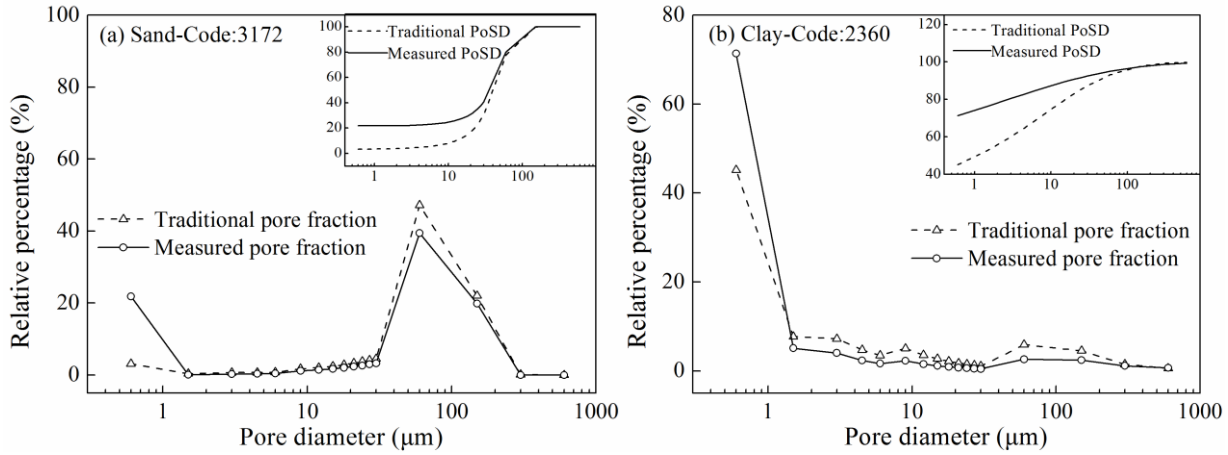
Figure 1: Measured vs. calculated pore volume fraction curves for (a) sand (code: 3172) and (b) clay (code: 2360). The measured and calculated PoSDs are embedded in the tops of the figures.
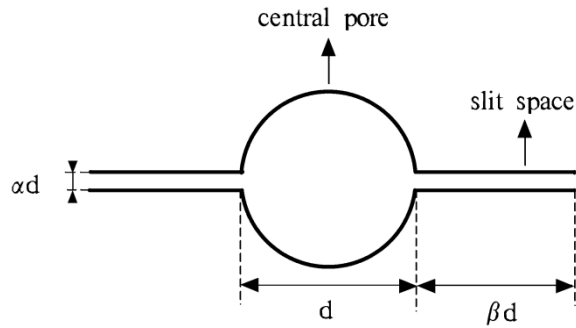
Figure 2: Pore space geometry model containing two slit-shaped spaces (d denotes the diameter of the central pore, and αd and βd denote the widths and lengths of the slit-shaped spaces, respectively).

	Formed pores	PSD	Volume fraction of slit–shaped spaces	Volume fraction of pores
$d_1 \leqslant 0.6\,\mu m$		ω_1		$v_1 = \omega_1 + \zeta_2 + \cdots + \zeta_i$
d_2		ω_2	ζ_2	$v_2 = \omega_2 - \zeta_2$
$\vdots$	$\vdots$	$\vdots$	$\vdots$	$\vdots$
d_i		ω_i	ζ_i	$v_i = \omega_i - \zeta_i$

Figure 3: Schematic of the procedure used to calculate the pore volume fraction.
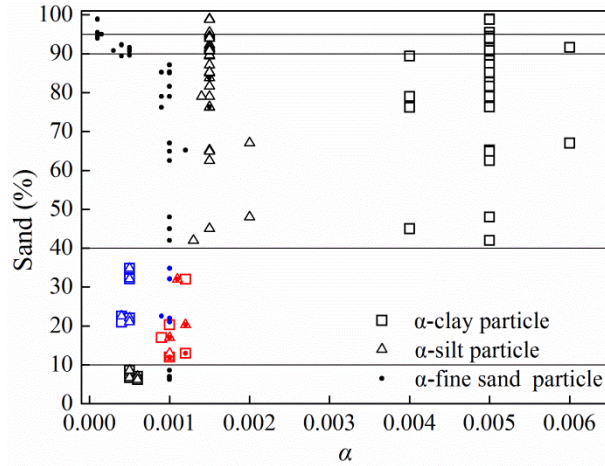
Figure 4: The α values for the 48 soil samples with different sand contents. The α values for specific samples of clay, silt, and fine

5   **sand are listed in Figure 4 except those of coarse sand particles, which are the same value of 0.0004 for all of the samples. For the samples with sand contents ranging from 10-40%, two sets of α values are observed. The α values for silt contents of less than and more than 50% are highlighted in red and blue, respectively, thereby reflecting the dominant functions of silt or clay particles on the hydraulic properties of the typical samples.**
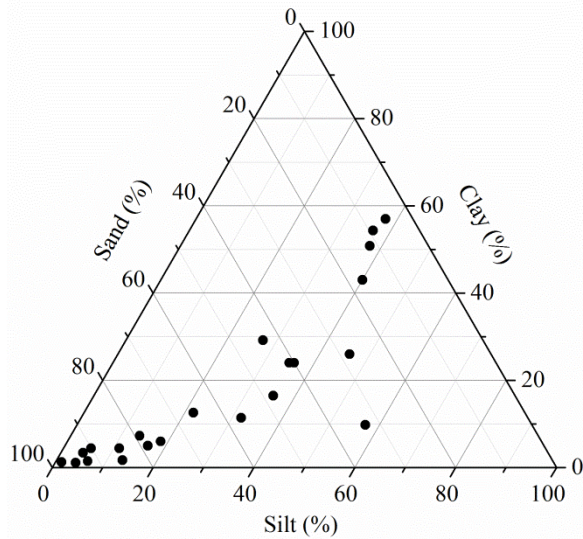
Figure 5: Textural distribution of the 22 soil samples for the model validation.

20
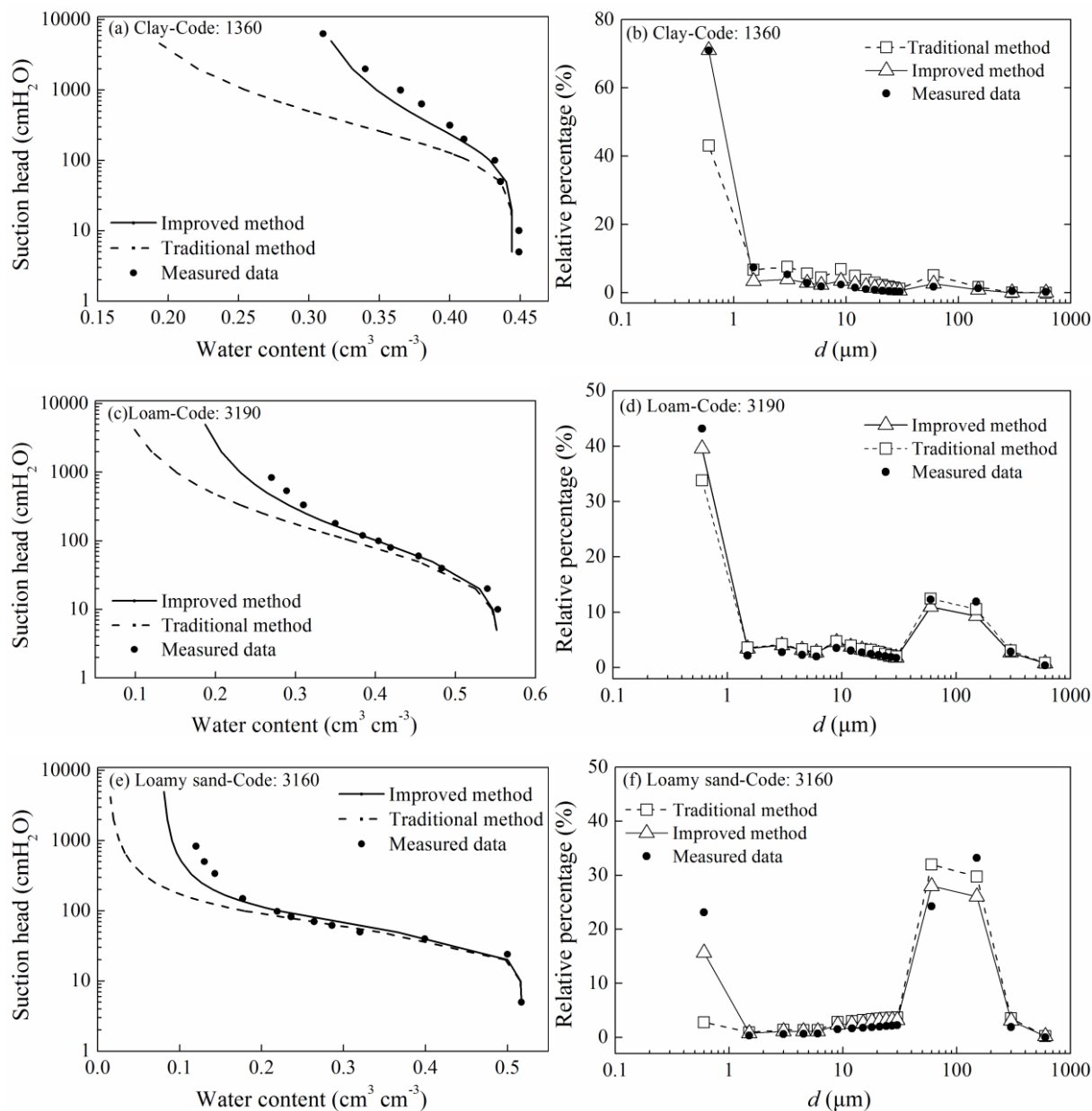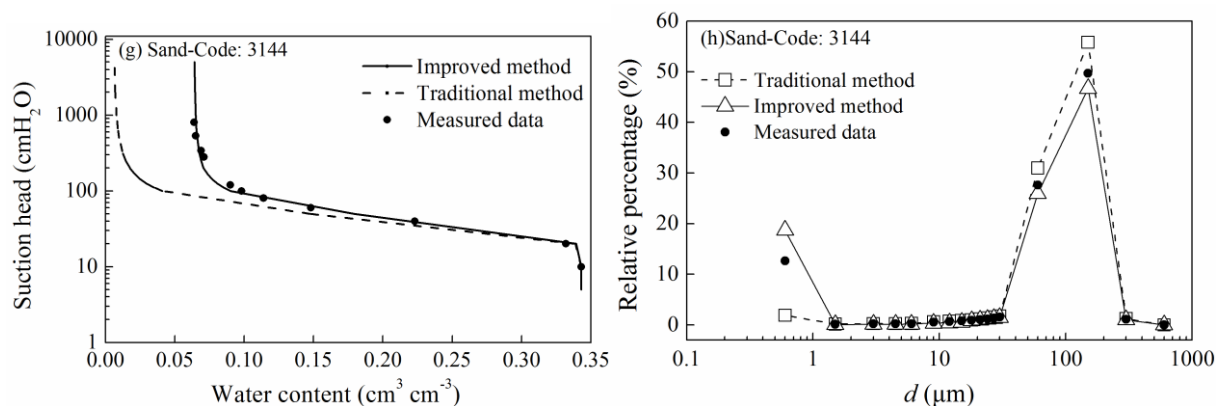
Figure 6: Measured and predicted SWC curves (left) in addition to measured and predicted pore volume fraction curves (right) for clay (code: 1360), loam (code: 3190), loamy sand (code: 3160) and sand (code: 3144).
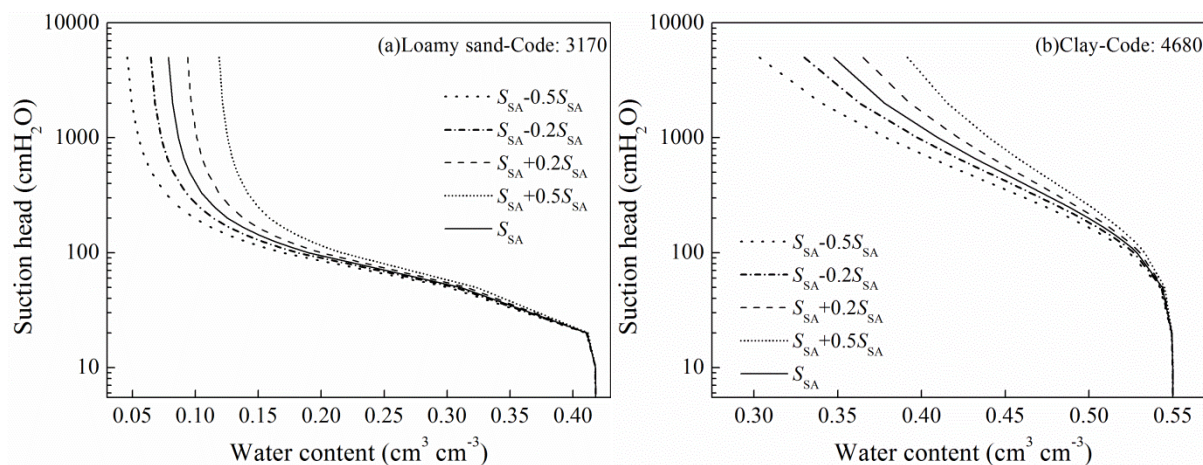
Figure 7: The effects of an alteration of the estimated S_{SA} on the SWC for (a) loamy sand (code: 3170) and (b) clay (code: 4680). S_{SA} denotes the accurate value of the specific surface area.

Loamy sand−Code: 3170		$S_{SA} = 8.19 m^2 g^{-1}$		
Particle size fraction	Formed pores	αd (m)	βd (m)	S_{SAi} ($m^2 g^{-1}$)
Clay	$d \leqslant 0.6 \mu m$	3E−9	0.00004	4.98
Silt	$0.6 \mu m < d \leqslant 15 \mu m$	1.4E−8	0.00056	1.91
Fine sand	$15 \mu m < d \leqslant 150 \mu m$	8.4E−8	0.0051	1.29
Coarse sand	$150 \mu m < d \leqslant 600 \mu m$	1.2E−7	0.0178	0.006

Figure 8: The calculated slit width αd, slit length βd and S_{SAi} for loamy sand (code: 3170).

Table 1: Codes and textural classes of the 48 soils selected from UNSODA

UNSODA codes	Textual class
4681, 4680, 2362, 2360, 1400, 1383, 4221, 1361, 2340	Clay
3191, 1091, 2530, 2531	Loam
2102, 3150, 3161, 3171, 1160, 3170, 3130, 1031, 4011, 4020	Loamy sand
1464, 1466, 2100, 3340, 4650, 3142, 1050, 1023, 3141, 3163, 3164, 3165, 3172, 4051, 4520, 4521	Sand
3202	Sandy clay loam
3200, 3203, 4162	Sandy loam
4042, 4180, 4070, 4673, 1341	Silt loam

Table 2: The estimated values of α for various soil textures

Sand content (%)	Silt content (%)	α			
		Clay $D \leq 2 \mu m$	Silt $2 \mu m < D \leq 50 \mu m$	Fine sand $50 \mu m < D \leq 500 \mu m$	Coarse sand $500 \mu m < D \leq 2000 \mu m$
0-10		0.0005	0.0005	0.001	0.0004
10-40	0-50	0.001	0.001	0.001	0.0004
	50-100	0.0005	0.0005	0.001	0.0004
40-90		0.005	0.0015	0.001	0.0004
90-95		0.005	0.0015	0.0005	0.0004
95-100		0.005	0.0015	0.0001	0.0004

Table 3: Codes of the 22 soil samples selected from UNSODA for the model validation

UNSODA codes	Textual class
1360, 4120, 2361, 3282	Clay
3190, 1370	Loam
3160, 3152, 1030, 1090, 4010	Loamy sand
3155, 3144, 1463, 3132, 4000	Sand
4620, 4621	Sandy clay loam
3290, 3310	Sandy loam
4531, 4510	Silt loam

5   **Table 4: The root mean square errors (E_{RMS}) of the SWC predicted using both the improved method and the traditional method**

Soil texture	Number of soil sample	E_{RMS}	
		Improved method	Traditional method
Clay	4	0.025	0.044
Loam	2	0.054	0.106
Loamy sand	5	0.020	0.048
Sand	5	0.017	0.042
Sandy clay loam	2	0.034	0.086
Sandy loam	2	0.046	0.068
Silt loam	2	0.024	0.040